



# Stability of the Artificial Equilibrium Points in the Low-Thrust Restricted Three-Body Problem when the Bigger Primary is a Source of Radiation

Md. Sanam Suraj<sup>1</sup>, Amit Mittal<sup>2</sup> and Krishan Pal<sup>3\*</sup>

<sup>1</sup> *Department of Mathematics, Sri Aurobindo College, University of Delhi, New Delhi, India*

<sup>2</sup> *Department of Mathematics, A.R.S.D. College, University of Delhi, New Delhi, India*

<sup>3</sup> *Department of Mathematics, Maharaja Agrasen College, University of Delhi, New Delhi, India*

Received: December 25, 2019; Revised: April 23, 2020

**Abstract:** This paper investigates the existence and the stability of artificial equilibrium points (AEPs) in the low-thrust restricted three-body problem when the bigger primary is a source of radiation and the smaller one is a point mass. The linear stability of the AEPs has been studied. Firstly, we have derived the equations of motion of the spacecraft in the synodic coordinate system. The AEPs are obtained by cancelling the gravitational and centrifugal forces with continuous control acceleration at the non-equilibrium points. The positions of these AEPs will depend on the magnitude and directions of low-thrust acceleration. Secondly, we have calculated the numerical values of the AEPs and their movement shown graphically for given thrust parameters. We have found the stability regions in the  $x - y$ ,  $x - z$ ,  $y - z$ -planes and studied the effect of the radiation pressure on the motion of the spacecraft. Further, we have drawn the zero velocity curves (ZVCs) to determine the possible regions of motion in which the spacecraft is free to move.

**Keywords:** *restricted three-body problem, artificial equilibrium points, low-thrust, stability, radiation pressure, zero velocity curves.*

**Mathematics Subject Classification (2010):** 70F07, 70F10, 70F15.

---

\* Corresponding author: <mailto:kp11987@gmail.com>

## 1 Introduction

The restricted three-body problem with many perturbing forces, like oblateness, radiation forces of the primaries, Coriolis and centrifugal forces have been studied by many scientists and researchers. There are five Lagrangian points in the classical restricted three-body problem (R3BP), three of them are on the straight line joining the primaries, called collinear libration points, and two of them set up equilateral triangle with the primaries. Szebehely [1] has investigated the five libration points. The collinear libration points  $L_{1,2,3}$  are always unstable in the linear sense for any value of the mass parameter  $\mu$ , whereas the triangular libration points  $L_{4,5}$  are stable if  $\mu < \mu_c = 0.03852$ . Kunitsyn and Perezhogin [2], Kumar and Choudhry [3], Abouelmagd [4], and Singh and Emmanuel [5] have studied the stability properties of the equilibrium points in the photogravitational R3BP. Zotos [6] has studied numerically the case of the planar circular photogravitational R3BP where the more massive primary is an emitter of radiation. He has found that the radiation pressure factor has a huge impact on the character of orbits. Srivastava et al. [7] have introduced the Kustaanheimo-Stiefel (KS)-transformation to reduce the order of singularities arising due to the motion of an infinitesimal body in the vicinity of the smaller primary in the R3BP when the bigger primary is a source of radiation and the smaller one is an oblate spheroid. They have found that the KS-regularization reduces the order of the pole from five to three at the point of singularity of the governing equations of motion. Correa et al. [8] introduced two models of the restricted three-body and four-body problems. They have investigated the transfer orbits from a parking orbit around the Earth to the halo orbit in both the dynamical models. Also, they have compared the total velocity increment to both the models. Prado [9] has worked on the space trajectories in the circular restricted three-body problem. Further, he assumed that the spacecraft moves under the gravitational forces of two massive bodies which are in circular orbits. He also investigated the orbits which can be used to transfer a spacecraft from one body back to the same body or to transfer a spacecraft from one body to the respective Lagrangian points  $L_4$  and  $L_5$ .

The Lagrangian points are only five positions in space where the small object if placed there, would maintain its position relative to the two massive bodies. If, however, the object is equipped with a suitable propulsion system, capable of balancing the gravitational pull of the two massive bodies, other equilibrium points can be generated allowing the third body to be stationary with respect to the first two bodies. According to Dusek [10] these new points are usually known as the Artificial Equilibrium Points (AEPs). Recently, low-thrust propulsion systems such as the solar sail and the electric propulsion systems are being developed not only for controlling satellite orbit, but also as main engines for interplanetary transfer orbits. These low-thrust propulsion systems are able to provide continuous control acceleration to the spacecraft and thus increase mission design flexibility. Describing the locations and investigating the stability conditions of the AEPs have been made by many authors. In particular, Farquhar [11] has studied the concept of telecommunication systems using the Lagrange points and investigated ballistic periodic orbits about these points in the Earth-Moon system. Simmons et al. [12] and Broschart and Scheeres [13] have studied the stability of equilibrium points with continuous control acceleration. Scheeres et al. [14] have analyzed a control law which stabilizes unstable periodic halo orbits about an Earth-Sun libration point with continuous acceleration taking hills problem and discussed applications to the spacecraft formation flight. Thereafter, many authors have been worked on the solar sails, see Morimoto et al. [15, 16], Baig and

McInnes [17], Bombardelli and Pelaez [18]. They have studied the stability of the artificial equilibrium points in the circular restricted three-body problem. Also, they have investigated the equilibrium points for hybrid low-thrust propulsion system. Bu et al. [19] have investigated the positions and dynamical characteristic of the AEPs in a binary asteroid system with continuous low-thrust. They have found the stable regions of the AEPs by a parametric analysis and studied the effect of the mass ratio and ellipsoid parameters on the stable region. Further, they have analyzed the effect of the continuous low-thrust on the feasible region of motion by ZVCs. More recently, Sushil et al. [20] have been studied the existence and stability of equilibrium points in the restricted three-body problem with a geo-centric satellite including the Earth’s equatorial ellipticity.

In the present paper, we have studied the effect of radiation pressure of the bigger primary on the motion of the spacecraft. This paper is an extension of the work of Morimoto et al. [15]. This paper is organized as follows. In Section 2, we have derived the equations of motion of the spacecraft. In Section 3, we have found the locations of the AEPs. In Section 4, we have found the stability conditions and stable regions. In Section 5, we have drawn the zero velocity curves. Finally, in Section 6, we have concluded the results obtained.

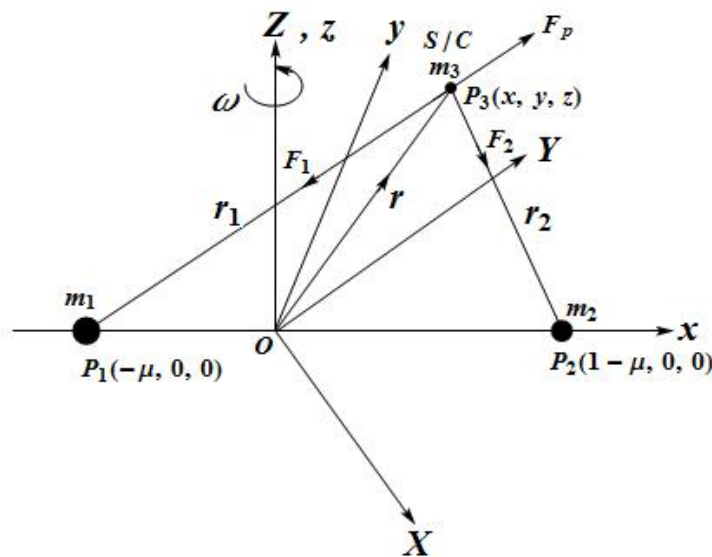


Figure 1: Configuration of the problem.

## 2 Equation of Motion

Let two celestial bodies of masses  $m_1$  and  $m_2$  ( $m_1 > m_2$ ) be the primaries moving with angular velocity  $\omega$  in circular orbits about their center of mass  $O$  taken as the origin, and let the infinitesimal body (a spacecraft) of mass  $m_3$  is moving in the plane of motion of  $m_1$  and  $m_2$ . The motion of the spacecraft is affected by the motion of  $m_1$  and  $m_2$  but without affecting their motion. In this problem, we assume that the bigger primary is a source of radiation and the smaller one is a point mass. The line joining the primaries

$m_1$  and  $m_2$  is taken as the  $X$ -axis, the line which passes through  $O$  and is perpendicular to the  $X$ -axis and lying in the plane of motion of  $m_1$  and  $m_2$  is considered as the  $Y$ -axis, and the line which passes through the origin and is perpendicular to the plane of motion of the primaries is taken as the  $Z$ -axis. We have taken the synodic system of coordinates  $O(xyz)$ , initially coincident with the inertial system of coordinates  $O(XYZ)$ , rotating with the angular velocity  $\omega$  about the  $z$ -axis (the  $z$ -axis is coincident with the  $Z$ -axis). A complete diagram of the formulated problem is shown in Figure 1. Let the primaries of masses  $m_1$  and  $m_2$  be located at  $P_1(-\mu, 0, 0)$  and  $P_2(1-\mu, 0, 0)$ , respectively, and the spacecraft is located at the point  $P_3(x, y, z)$  (see Fig. 1). The angular velocity of the primaries is given by the relation  $\omega = \sqrt{\frac{G(m_1+m_2)}{l^3}}$ , where  $l$  is the distance between the primaries, and  $G$  is the gravitational constant. We scale the units by taking the sum of the masses and the distance between the primaries both equal to unity. Therefore,  $m_1 = 1 - \mu$ ,  $m_2 = \mu$ ,  $\mu = \frac{m_2}{m_1+m_2}$  and  $\mu \in (0, 0.5]$  with  $m_1 + m_2 = 1$ . The scale of time is chosen so that the gravitational constant is unity and thus, the angular velocity of the primaries is one. The equation of motion of the spacecraft in vector form is expressed as

$$\frac{d^2\mathbf{r}}{dt^2} + 2\boldsymbol{\omega} \times \frac{d\mathbf{r}}{dt} = \mathbf{a} - \nabla\Omega = \mathbf{F}, \quad (1)$$

where  $\Omega$  is the effective potential of the system that combines the gravitational potential and the potential from the centripetal acceleration, and which is given by

$$\Omega = -\frac{n^2}{2}(x^2 + y^2) - \frac{q(1-\mu)}{r_1} - \frac{\mu}{r_2},$$

and

$$\begin{aligned} \mathbf{F} &= \text{the total force acting on } m_3 \\ &= \mathbf{F}_1 + \mathbf{F}_2, \\ \mathbf{F}_1 &= \text{the gravitational force exerted on } m_3 \text{ due} \\ &\quad \text{to } m_1 \text{ along } \mathbf{P}_3\mathbf{P}_1, \\ \mathbf{F}_2 &= \text{the gravitational force exerted on } m_3 \text{ due} \\ &\quad \text{to } m_2 \text{ along } \mathbf{P}_3\mathbf{P}_2. \end{aligned}$$

The vector  $\mathbf{a} = (a_x, a_y, a_z)$  is the low-thrust acceleration and  $\mathbf{r} = (x, y, z)^T$  is the position vector of the spacecraft. Thus, the equations of motion of the spacecraft with continuous low-thrust in the dimensionless co-ordinate system can be written as

$$\left. \begin{aligned} \ddot{x} - 2n\dot{y} &= -\Omega_x + a_x = -\Omega_x^*, \\ \ddot{y} + 2n\dot{x} &= -\Omega_y + a_y = -\Omega_y^*, \\ \ddot{z} &= -\Omega_z + a_z = -\Omega_z^*, \end{aligned} \right\} \quad (2)$$

where

$\Omega^*$  is the potential of the system with continuous low-thrust that can be written as

$$\Omega^* = \Omega - \mathbf{a} \cdot \mathbf{r} = \Omega - a_x x - a_y y - a_z z,$$

$$= -\frac{n^2}{2}(x^2 + y^2) - \frac{q(1-\mu)}{r_1} - \frac{\mu}{r_2} - a_x x - a_y y - a_z z,$$

where

$$r_1 = \sqrt{(x + \mu)^2 + y^2 + z^2}, \quad r_2 = \sqrt{(x + \mu - 1)^2 + y^2 + z^2},$$

and

$$q = 1 - \frac{F_p}{F_g} = 1 - p,$$

$q$  = the radiation parameter,

$p$  = the radiation pressure,

$F_g$  = the gravitational attraction force due to the bigger primary  $m_1$ ,

$F_p$  = the radiation pressure due to bigger primary  $m_1$ ,

$n$  is the mean motion of the primaries whose value is one in this problem. The magnitude of control acceleration is given by

$$a = \sqrt{a_x^2 + a_y^2 + a_z^2}.$$

### 3 The Locations of Artificial Equilibrium Points

The AEPs are the solutions of the equations  $\Omega_x^* = 0, \Omega_y^* = 0, \Omega_z^* = 0$ . In order to find the AEPs of the system, take the velocity and acceleration of the system equal to 0, i.e.,  $\dot{x} = \dot{y} = \dot{z} = 0, \ddot{x} = \ddot{y} = \ddot{z} = 0$ . The AEPs denoted by  $(x_0, y_0, z_0)$  are the solution of the equations given by

$$\left. \begin{aligned} -x_0 + \frac{q(1-\mu)}{r_1^3}(x_0 + \mu) + \frac{\mu}{r_2^3}(x_0 - \mu_1 - 1) - a_x &= 0, \\ -y_0 + \frac{q(1-\mu)}{r_1^3}y_0 + \frac{\mu}{r_2^3}y_0 - a_y &= 0, \\ \frac{q(1-\mu)}{r_1^3}z_0 + \frac{\mu}{r_2^3}z_0 - a_z &= 0. \end{aligned} \right\} \quad (3)$$

The AEPs which lie on the  $x$ -axis are called collinear and are obtained from Eqs. (3) by taking  $y = z = 0$ . The AEPs which lie in the  $xy$ -plane but not on the  $x$ -axis are called non-collinear. We have obtained five AEPs denoted by  $L_1, L_2, L_3, L_4$  and  $L_5$  for given parameters. In Tables 1 and 2, we have presented the numerical values of a few AEPs for the fixed values of  $\mu = 0.1, q = 0.99$  and varying  $\mathbf{a}$  in the  $x$ -direction. From Tables 1 and 2, we have observed that there exist three collinear and two non-collinear AEPs.

The locations of the collinear and non-collinear AEPs are shown in Fig. 2 for the different values of the radiation parameter  $q(0 < q < 1)$  and low-thrust acceleration  $\mathbf{a} = (a_x, 0, 0)$ . From Fig. 2 (a), we have observed that when  $\mathbf{a} = (a_x, 0, 0)$  is increasing, the AEPs  $L_1, L_2$  and  $L_3$  have almost negligible movement, the AEPs  $L_4$  and  $L_5$  move towards the  $y$ -axis, and we have noticed that the non-collinear AEPs  $L_4$  and  $L_5$  are symmetric about the  $x$ -axis. From Fig. 2 (b), we have observed that when  $q$  is increasing, all the AEPs are going away from the primary  $m_1$  and the AEPs  $L_4$  and  $L_5$  are symmetric about the  $x$ -axis. We have also observed that the AEPs are the new positions of the equilibrium points with the effect of the continuous low-thrust  $\mathbf{a}$  and radiation parameter  $q$ , these points are different from the natural libration points.

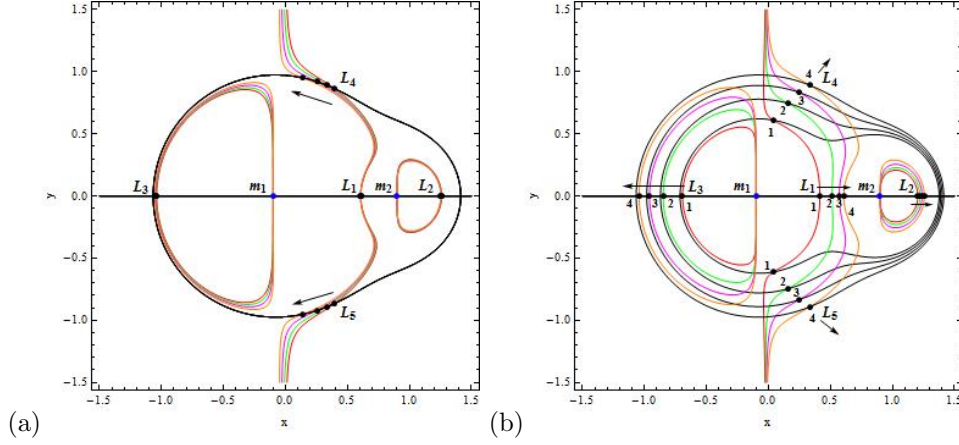


**Figure 2:** The locations of the five AEPs in the low-thrust R3BP with the effect of radiation pressure for  $\mu = 0.1$ . (a) For  $q = 0.99$  and for  $\mathbf{a} = (0.0001, 0, 0)$  (black, red),  $(0.015, 0, 0)$  (black, green),  $(0.03, 0, 0)$  (black, magenta),  $(0.045, 0, 0)$  (black, orange). (b) For  $\mathbf{a} = (0.015, 0, 0)$  and for  $q = 0.25$  (black, red),  $0.50$  (black, green),  $0.75$  (black, magenta),  $0.99$  (black, orange).

$\mu = 0.1$				
$q = 0.99$				
$\mathbf{a}$	$L_1$	$L_2$	$L_3$	$L_{4,5}$
$\mathbf{a} = 0.0001$	(0.607756, 0)	(1.25887, 0)	(-1.03844, 0)	(0.396291, $\pm 0.864259$ )
$\mathbf{a} = 0.0150$	(0.606693, 0)	(1.25643, 0)	(-1.04315, 0)	(0.334002, $\pm 0.891111$ )
$\mathbf{a} = 0.0300$	(0.605617, 0)	(1.25400, 0)	(-1.04793, 0)	(0.251705, $\pm 0.920949$ )
$\mathbf{a} = 0.0450$	(0.604536, 0)	(1.25161, 0)	(-1.05276, 0)	(0.135929, $\pm 0.951772$ )

**Table 1:** The AEPs in the  $xy$ -plane when  $\mathbf{a}$  is varying in the  $x$ -direction.

$\mu = 0.1$				
$\mathbf{a} = 0.015$				
$q$	$L_1$	$L_2$	$L_3$	$L_{4,5}$
$q = 0.25$	(0.413878, 0)	(1.20345, 0)	(-0.693390, 0)	(0.039034, $\pm 0.610877$ )
$q = 0.50$	(0.513221, 0)	(1.21998, 0)	(-0.849261, 0)	(0.154312, $\pm 0.747250$ )
$q = 0.75$	(0.570035, 0)	(1.23791, 0)	(-0.958911, 0)	(0.251001, $\pm 0.832607$ )
$q = 0.99$	(0.606693, 0)	(1.25643, 0)	(-1.043150, 0)	(0.334002, $\pm 0.891111$ )

**Table 2:** The AEPs in the  $xy$ -plane when  $q$  is varying and  $\mathbf{a} = (0.015, 0, 0)$ .

#### 4 Stability Analysis and Stable Regions

To establish the spacecraft at a non-equilibrium point, a continuous low-thrust is provided to the spacecraft. Now, give the small displacement to  $(x_0, y_0, z_0)$  as  $x = x_0 + \delta_x$ ,  $y =$

$y_0 + \delta_y, z = z_0 + \delta_z, (\delta_x, \delta_y, \delta_z \ll 1)$ . Using the above displacements, the linearized equations of motion (according to Morimoto et al. [16]) corresponding to Eqs. (2) are given by

$$\left. \begin{aligned} \ddot{\delta}_x - 2n\dot{\delta}_y &= \Omega_{xx}^0 \delta_x + \Omega_{xy}^0 \delta_y + \Omega_{xz}^0 \delta_z, \\ \dot{\delta}_y + 2n\dot{\delta}_x &= \Omega_{yx}^0 \delta_x + \Omega_{yy}^0 \delta_y + \Omega_{yz}^0 \delta_z, \\ \ddot{\delta}_z &= \Omega_{zx}^0 \delta_x + \Omega_{zy}^0 \delta_y + \Omega_{zz}^0 \delta_z, \end{aligned} \right\} \quad (4)$$

where the superscript “0” overhead in Eqs. (4) indicates that the values are to be calculated at the AEP  $(x_0, y_0, z_0)$  under consideration. The characteristic root  $\lambda$  satisfies the given characteristic equation

$$\left. \begin{aligned} \lambda^6 + (\Omega_{xx}^0 + \Omega_{yy}^0 + \Omega_{zz}^0 + 4) \lambda^4 + (\Omega_{xx}^0 \Omega_{yy}^0 + \Omega_{xx}^0 \Omega_{zz}^0 + \Omega_{yy}^0 \Omega_{zz}^0 - (\Omega_{xy}^0)^2 \\ - (\Omega_{xz}^0)^2 - (\Omega_{yz}^0)^2 + 4\Omega_{zz}^0) \lambda^2 + \Omega_{xx}^0 \Omega_{yy}^0 \Omega_{zz}^0 + 2 \Omega_{xy}^0 \Omega_{xz}^0 \Omega_{yz}^0 - (\Omega_{xy}^0)^2 \Omega_{zz}^0 \\ - (\Omega_{xz}^0)^2 \Omega_{yy}^0 - (\Omega_{yz}^0)^2 \Omega_{xx}^0 = 0. \end{aligned} \right\} \quad (5)$$

If  $k = \lambda^2$ , we obtain

$$\left. \begin{aligned} k^3 + (\Omega_{xx}^0 + \Omega_{yy}^0 + \Omega_{zz}^0 + 4) k^2 + (\Omega_{xx}^0 \Omega_{yy}^0 + \Omega_{xx}^0 \Omega_{zz}^0 + \Omega_{yy}^0 \Omega_{zz}^0 - (\Omega_{xy}^0)^2 \\ - (\Omega_{xz}^0)^2 - (\Omega_{yz}^0)^2 + 4\Omega_{zz}^0) k + \Omega_{xx}^0 \Omega_{yy}^0 \Omega_{zz}^0 + 2 \Omega_{xy}^0 \Omega_{xz}^0 \Omega_{yz}^0 - (\Omega_{xy}^0)^2 \Omega_{zz}^0 \\ - (\Omega_{xz}^0)^2 \Omega_{yy}^0 - (\Omega_{yz}^0)^2 \Omega_{xx}^0 = 0. \end{aligned} \right\} \quad (6)$$

The Eqn. (6) is a cubic equation in  $k$  that can be written as

$$k^3 + d_1 k^2 + d_2 k + d_3 = 0, \quad (7)$$

where

$$\begin{aligned} d_1 &= \Omega_{xx}^0 + \Omega_{yy}^0 + \Omega_{zz}^0 + 4 = 1, \\ d_2 &= \Omega_{xx}^0 \Omega_{yy}^0 + \Omega_{xx}^0 \Omega_{zz}^0 + \Omega_{yy}^0 \Omega_{zz}^0 - (\Omega_{xy}^0)^2 - (\Omega_{xz}^0)^2 - (\Omega_{yz}^0)^2 + 4\Omega_{zz}^0, \\ d_3 &= \Omega_{xx}^0 \Omega_{yy}^0 \Omega_{zz}^0 + 2 \Omega_{xy}^0 \Omega_{xz}^0 \Omega_{yz}^0 - (\Omega_{xy}^0)^2 \Omega_{zz}^0 - (\Omega_{xz}^0)^2 \Omega_{yy}^0 - (\Omega_{yz}^0)^2 \Omega_{xx}^0. \end{aligned}$$

Now, we determine the linear stability of the AEPs by finding the characteristic roots of Eqn. (7). We know that all the characteristic roots of a cubic equation are either real numbers or one of them is a real number and the other characteristic roots are imaginary numbers. According to the stability theory, a necessary and sufficient condition for an AEP to be linearly stable is that all the characteristic roots of Eqn. (5) lie in the left-hand side of the  $\lambda$ -plane (i.e.,  $\lambda \leq 0$ ). If one or more characteristic roots of Eqn. (5) lie in the right-hand side of the  $\lambda$ -plane, then the AEP is always unstable. If all the characteristic roots of Eqn. (5) lie to the left-hand side of the  $\lambda$ -plane, then Eqn. (7) must have three real and negative roots. The resulting linear stability conditions according to Morimoto et al. [16] and Descartes’s sign rule often are  $D \geq 0, d_2 > 0$  and  $d_3 > 0$ , where  $D$  is the discriminant of the cubic Eqn. (7) and is given by

$$D = \frac{1}{4} \left( d_3 + \frac{16 - 18 d_2}{27} \right)^2 + \frac{1}{27} \left( d_2 - \frac{4}{3} \right)^3. \quad (8)$$

Finally, it is concluded that the system of AEPs is linearly stable when  $D \geq 0$ ,  $d_2 > 0$  and  $d_3 > 0$ .

Further, we have plotted the stability regions in the  $x - y$ ,  $x - z$  and  $y - z$ -planes as shown in Fig. 3. The gray areas in Figs. 3 indicate the stability regions of the AEPs satisfying the stability conditions  $D \geq 0$ ,  $d_2 > 0$  and  $d_3 > 0$ . From Fig. 3 (a, b), we have observed that the stability regions reduce around  $m_2$  and expand around  $m_1$  for the increasing values of radiation parameter  $q$  ( $0 < q < 1$ ). Further, from Fig. 3 (c, d, e, f), we have observed that the stability regions increase around both the primaries  $m_1$  and  $m_2$  for the increasing values of radiation parameter  $q$  ( $0 < q < 1$ ).

## 5 Zero Velocity Curves

The Jacobian integral of the equations of motion in the classical system is defined as

$$C = 2\Omega + (\dot{x}^2 + \dot{y}^2 + \dot{z}^2). \quad (9)$$

The Jacobian integral of the equations of motion with the continuous low-thrust is defined as

$$C' = 2\Omega^* + (\dot{x}^2 + \dot{y}^2 + \dot{z}^2). \quad (10)$$

We have plotted the ZVCs by taking  $\dot{x} = \dot{y} = \dot{z} = 0$ . The white domains correspond to the Hills region, and the cyan color indicates the forbidden regions, while the thick black lines show the ZVCs. In these ZVCs, the black dots indicate the positions of the AEPs, while the blue dots indicate the positions of two primaries.

In Figs. 4, we have plotted the ZVCs for the fixed values of  $\mu = 0.1$ ,  $q = 0.99$ ,  $C' = -3.57174$  and for different values of low-thrust acceleration  $\mathbf{a}$ . Fig. 4 (a) indicates the ZVC for the low-thrust acceleration  $\mathbf{a} = (0.0001, 0, 0)$  and shows that there exists a circular land (white domains) around both the primaries and the spacecraft is trapped in these regions, where the motion is possible, and the circular strip (the cyan color) shows the forbidden region where the motion is not possible. Thus, the spacecraft can move around both the primaries and can not move from one primary to the other primary.

In Fig. 4 (b), as we have increased the value of the low-thrust acceleration  $\mathbf{a} = (0.15, 0, 0)$ , it is observed that the spacecraft can freely move in the entire white domain. In Fig. 4 (c), there exist a limiting situation for  $\mathbf{a} = (0.245, 0, 0)$  and a cusp at  $L_3$ , it is observed that the spacecraft can freely move in the entire white domain. In Fig. 4 (d), the curves of zero velocity constitute two branches for  $\mathbf{a} = (0.335, 0, 0)$ . The first branch contains  $L_4$  and the other branch contains  $L_5$ . Also, the curves split into two parts at  $L_3$  and shrink to the tadpole shaped curves around  $L_4$  and  $L_5$ . Hence, there is only forbidden region around  $L_4$  and  $L_5$  in the tadpole shaped region and the spacecraft is free to move everywhere in the plane.

## 6 Conclusion

In this paper, we have studied the existence and stability of the AEPs in the low-thrust R3BP when the bigger primary is a source of radiation and the smaller one is a point mass. The AEPs are obtained by introducing the continuous low-thrust at the non-equilibrium points. The positions of these AEPs will depend on the magnitude and directions of the low-thrust acceleration. We have calculated a few AEPs numerically as shown in

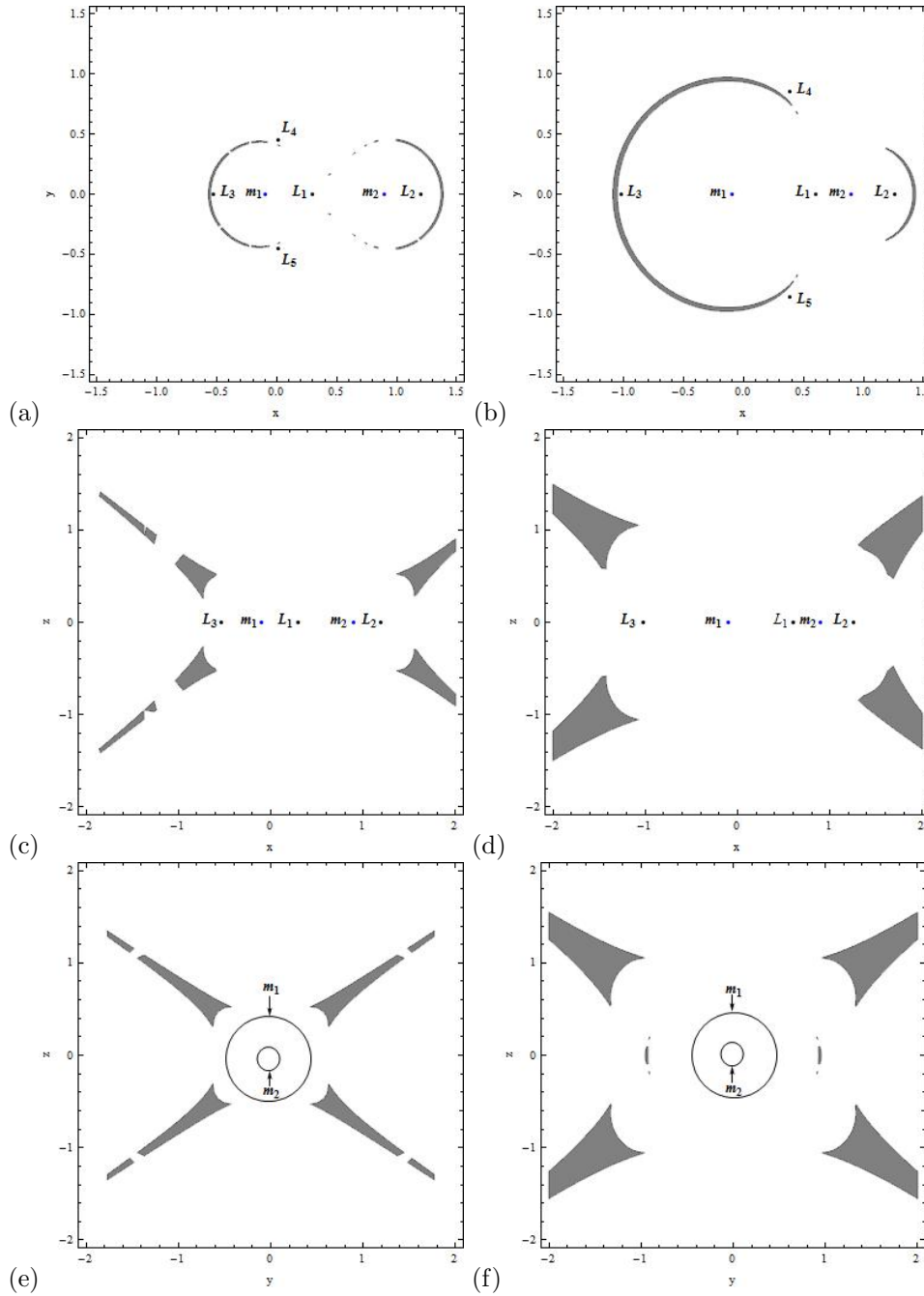


**Figure 3:** The stable regions (gray area) in the low-thrust R3BP with the effect of the radiation pressure  $q$  ( $0 < q < 1$ ) for fixed value of the mass parameter  $\mu = 0.1$ . (a, b) In the  $x - y$ -plane for  $q = 0.1, 0.95$ , respectively; (c, d) In the  $x - z$ -plane for  $q = 0.1, 0.95$ , respectively; (e, f) In the  $y - z$ -plane for  $q = 0.1, 0.95$ , respectively.

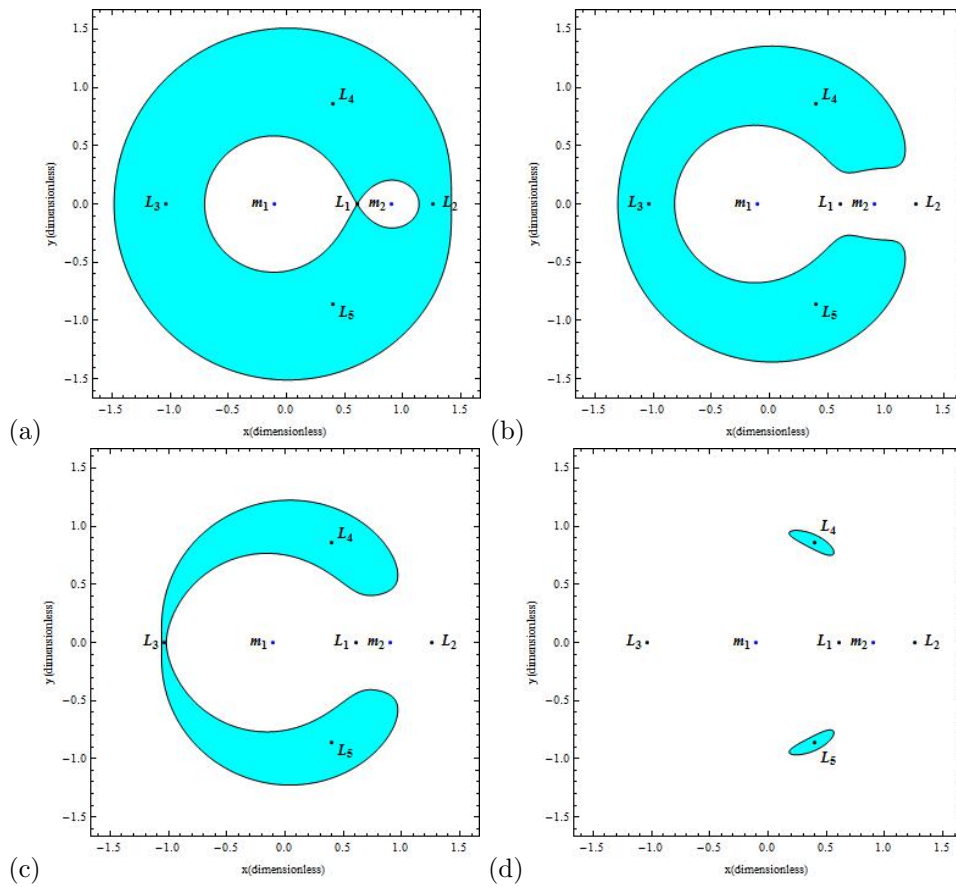


**Figure 4:** The ZVCs in the low-thrust R3BP for the fixed values of  $\mu = 0.1$ ,  $q = 0.99$  and for different values of the low-thrust acceleration  $a$ .

Tables 1 and 2. From Tables 1 and 2, we have observed that there exist three collinear and two non-collinear AEPs. It is noticed that the non-collinear AEPs  $L_4$  and  $L_5$  are symmetric about the  $x$ -axis for the varying low-thrust acceleration in the  $x$ -direction. The movement of the AEPs is shown graphically and displayed in Figs. 2 with the effect of the radiation and low-thrust parameters. It is found that the radiation parameter has more impact on the positions of the AEPs. In our case, the positions of the AEPs are different from those in Morimoto et al. [16], Baig and McInnes [17] and Bu et al. [19] due to the presence of the radiation parameter  $q$  ( $0 < q < 1$ ) of the bigger primary. But the positions of these AEPs can be similar to those in the works of Morimoto et al. [16], Baig and McInnes [17], and Bu et al. [19] when  $q = 1$  and  $\mathbf{a} \neq (0, 0, 0)$ .

Next, the effect of the radiation parameter  $q$  ( $0 < q < 1$ ) is studied on stable regions of the spacecraft. From Figs. 3 (a, b), we have observed that the stable regions reduce around the second primary  $m_2$  and expand around the first primary  $m_1$  for the increasing values of the radiation parameter  $q$  ( $0 < q < 1$ ) and for a fixed value of the mass parameter  $\mu = 0.1$ . Further, from Figs. 3 (c, d, e, f), we have observed that the stable regions in the  $x - z$  and  $y - z$ -planes increase for the increasing values of the radiation parameter  $q$  ( $0 < q < 1$ ) and for a fixed value of the mass parameter  $\mu = 0.1$ . We have observed that the stability regions are different from those in Morimoto et al. [16] and Bu et al. [19] when  $q$  ( $0 < q < 1$ ) is effective. When  $\mathbf{a} = (0, 0, 0)$  and  $q = 1$ , the obtained results are in agreement with those by Szebehely [1]. Furthermore, from Figs. 3, it is also observed that the AEPs which lie in the stable regions (gray areas) will be linearly stable and otherwise unstable.

Finally, in Figs. 4, we have drawn the ZVCs. It is concluded that for different values of the low-thrust acceleration  $\mathbf{a}$  and for a fixed value of the mass parameter  $\mu = 0.1$ , we have different trapped areas in which the spacecraft can freely move. It is clear that the low-thrust acceleration  $\mathbf{a}$  has subsequent impact on the regions where the spacecraft can move.

### Acknowledgment

We are very thankful to the *Centre of Fundamental Research in Space Dynamics and Celestial Mechanics (CFRSC)*, New Delhi, India, for giving some necessary study materials and other supporting things which are required for the present research work.

### References

- [1] V. Szebehely. Theory of orbits, the restricted problem of three-bodies. *Academic press*. New York, 1967.
- [2] A. L. Kunitsyn and A. A. Perezhogin. On the stability of triangular libration points of the photogravitational restricted circular three-body problem. *Celest. Mech. Dyn. Astron.* **18**(4) (1978) 395–408.
- [3] V. Kumar and R. K. Choudhry. Nonlinear stability of the triangular libration points for the photo gravitational elliptic restricted problem of three bodies. *Celest. Mech. Dyn. Astron.* **48**(4) (1990) 299–317.
- [4] E. I. Abouelmagd. The effect of photogravitational force and oblateness in the perturbed restricted three-body problem. *Astrophys. Space Sci.* **346**(1) (2013) 51–69.
- [5] J. Singh and A. B. Emmanuel. Stability of triangular points in the photogravitational CR3BP with Poynting-Robertson drag and a smaller triaxial primary. *Astrophys. Space Sci.* **353** (1) (2014) 97–103.

- [6] E. E. Zotos. Unveiling the influence of the radiation pressure in nature of orbits in the photogravitational restricted three-body problem. *Astrophys. Space Sci.* **360** (1) (2015). Doi.10.1007/s10509-015-2513-2.
- [7] V. K. Srivastava, J. Kumar and B. S. Kushvah. Regularization of circular restricted three-body problem accounting radiation pressure and oblateness. *Astrophys. Space Sci.* **362** (49) (2017). Doi.10.1007/s10509-017-3021-3.
- [8] A. A. Correa, A. Prado, T. J. Stuchi and C. Beauge. Comparison of transfer orbits in the restricted three and four-body problems. *Nonlinear Dynamics and Systems Theory* **7** (3) (2007) 267–277.
- [9] A. F. B. A. Prado. A survey on space trajectories in the model of three-bodies. *Nonlinear Dynamics and Systems Theory* **6** (4) (2006) 389–400.
- [10] H. M. Dusek. Motion in the vicinity of libration points of a generalized restricted three-body model. *Prog. Astronaut. Rocket.* **17** (1966) 37–54.
- [11] R. W. Farquhar. Lunar communications with libration point satellites. *Spacecraft and Rockets.* **4** (10) (1967) 1383–1384.
- [12] J. F. L. Simmons, A. J. C. McDonald and J. C. Brown. The restricted three-body problem with radiation pressure. *Celest. Mech. Dyn. Astron.* **35** (1985) 145–187.
- [13] S. B. Broschart and D. J. Scheeres. Control of hovering spacecraft near small bodies: Application to Asteroid 25143 Itokwa. *J. Guid. Control Dyn.* **28** (2) (2005) 343–354.
- [14] D. J. Scheeres, F. Y. Hsiao and N. X. Vinh. Stabilizing motion relative to an unstable orbit: Application to spacecraft formation flight. *J. Guid. Control Dyn.* **26** (1) (2003) 62–73.
- [15] M. Y. Morimoto, H. Yamakawa and K. Uesugi. Periodic Orbits with low-thrust restricted three-body problem. *J. Guid. Control Dyn.* **29** (5) (2006) 1131–1139.
- [16] M. Y. Morimoto, H. Yamakawa and K. Uesugi. Artificial equilibrium points in the low-thrust restricted three-body problem. *J. Guid. Control Dyn.* **30** (5) (2007) 1563–1567.
- [17] S. Baig and C. R. McInnes. Artificial three-body equilibria for hybrid low-thrust propulsion. *J. Guid. Control Dyn.* **31** (6) (2008) 1644–1655.
- [18] C. Bombardelli and J. Pelaez. On the stability of artificial equilibrium points in the circular restricted three-body problem. *Celest. Mech. Dyn. Astron.* **109** (1) (2011) 13–26. Doi.10.1007/s10569-010-9317.
- [19] Shichao. Bu, Li. Shuang and Yang. Hongwei. Artificial equilibrium points in binary asteroid systems with continuous low-thrust. *Astrophys. Space Sci.* **362** (137) (2017). Doi.10.1007/s10509-017-31197-7.
- [20] S. Yadav, V. Kumar and R. Aggarwal. Existence and stability of equilibrium points in the restricted three-body problem with a Geo-Centric satellite including the Earth's equatorial ellipticity. *Nonlinear Dynamics and Systems Theory* **19** (4) (2019) 537–550.